

# PHYSICAL REVIEW B

## CONDENSED MATTER

THIRD SERIES, VOLUME 27, NUMBER 11

1 JUNE 1983

### Ionic conductivity and nuclear-magnetic-resonance study of fluorite-structured $K_{0.4}Bi_{0.6}F_{2.2}$

A. Cassanho,\* H. Guggenheim, and R. E. Walstedt  
*Bell Laboratories, Murray Hill, New Jersey 07974*

(Received 27 December 1982)

The (presumably ionic) electrical conductivity  $\sigma$  of  $K_{0.4}Bi_{0.6}F_{2.2}$  single crystals has been measured as a function of temperature, yielding Arrhenius-type behavior over a temperature range of  $\sim 300^\circ\text{C}$  with an activation energy of 0.389 eV. Doping the crystals with  $\text{Th}^{4+}$  and  $\text{Pb}^{2+}$  is found to increase  $\sigma$ , whereas  $\text{O}^{2-}$  is found to decrease  $\sigma$ . Nuclear-spin-echo decay times  $T_2$  give evidence that the conductivity is strongly inhomogeneous, in accordance with the disordered nature of this compound.

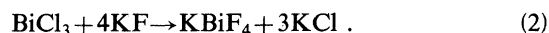
#### INTRODUCTION

Fluorite-structured binary compounds, in particular  $\beta\text{-PbF}_2$ , have recently been the subject of a relatively large number of investigations.<sup>1-7</sup> Ternary compounds with the fluorite structure present at room temperature (RT) a much higher ionic conductivity than the binary compounds due to their built-in defect structure. However, these materials have scarcely been studied up to now. In the present work, pure and doped potassium bismuth fluoride were grown as single crystals and their electrical conductivity was measured for temperatures ranging from RT to  $\sim 410^\circ\text{C}$ . Measurements of  $^{19}\text{F}$  nuclear-spin relaxation times  $T_1$  and  $T_2$ , taken over a wide range of temperatures, are also reported. These data are found to yield an interesting insight into the inhomogeneous nature of the conduction process. A phase transition observed in the conductivity results was also detected by differential thermal analysis (DTA).

#### SYNTHESIS AND CRYSTAL GROWTH

Potassium bismuth fluoride was precipitated from aqueous solution as follows: Bi metal ( $> 99.999\%$  purity) was dissolved in  $\text{HCl}:\text{HNO}_3$  5:1 solution and evaporated (by heating) to a viscous liquid which became a solid when cooled to room temperature. The  $\text{BiCl}_3$  solid was then dissolved in dilute HCl. The

concentration of HCl was just high enough to prevent the precipitation of  $\text{BiOCl}$ . In a large Teflon beaker a quantity of KF was dissolved in water and heated. The amount of KF was based on the weight of Bi metal as follows:



Reaction (2) was completed by slowly adding the  $\text{BiCl}_3$  solution from a separatory funnel into the KF solution while agitating with a magnetic stirrer. The insoluble potassium bismuth fluoride precipitate was then separated from the soluble KCl (and any slight excess of  $\text{BiCl}_3$ ) by vacuum filtration through a Buchner funnel using a fast filter paper (Whatman no. 4). The filtered white cake was then washed with acidified water and vacuum filtered. This was repeated three times using ethyl alcohol for the last wash. The dried material was stored over calcium sulfate desiccant and dried to constant weight.

Single crystals were grown from the melt by the horizontal zone technique and the Bridgman method. Most of the samples used for conductivity measurements were cut from zone-grown material. We found this method more suitable because the zone refining produced crystals of higher purity as evidenced by the gradual removal of light scattering after several passes. In addition, this method is also better for doping. Growth rates ranged from 0.3 to 1.0 cm/h.

### COMPOUND CHARACTERIZATION

The adopted synthesis method actually yielded a compound poor in KF. The lattice constant of the compound as obtained by Guinier-Hagg diffractometry was  $a = 5.907 \pm 0.003 \text{ \AA}$ . It was observed by Matar *et al.*<sup>8</sup> that the fluorite-structured solid solution  $K_{1-x}Bi_xF_{2x+1}$  ( $0.50 \leq x \leq 0.70$ ) obeys Vegard's law; according to their data our compound should be  $K_{0.39}Bi_{0.61}F_{2.22}$ . Chemical analysis of a succession of samples yielded results which were consistently within experimental error of  $K_{0.4}Bi_{0.6}F_{2.2}$ , in agreement with the proportions deduced from x-ray data. Since the ions  $K^+$  and  $Bi^{3+}$  occupy randomly the cation sites in the fluorite structure, one expects that the crystals will be strongly disordered on a microscopic scale because of local charge compensation.

### ELECTRICAL CONDUCTIVITY

The resistance of pure and doped samples was measured by a pulsed technique<sup>9</sup> using a 50- $\Omega$  standard resistor. The samples were spring loaded

between two platinum electrodes in a platinum conductivity cell. The electrical contacts were provided by colloidal graphite (Aquadag) and grafoil. A constant flow of purified nitrogen was maintained in the cell during the measurements.

The results for the pure crystal and three doped samples are shown in the form of plots  $\log_{10}(\sigma T)$  vs  $1000/T$  in Fig. 1. Table I gives the values of the prefactor  $\sigma_0$  and the apparent activation energy  $Q$ , assuming that  $\sigma$  can be represented by the equation:

$$\sigma = nZe u = \frac{\sigma_0}{T} \exp(-Q/k_B T).$$

Here  $n$  denotes the number of mobile defects per  $\text{cm}^3$ ,  $u$  is the mobility of the mobile defect, and  $Ze$  is the mobile-defect effective charge. The other symbols have their usual meanings. Comparing our results with the results for  $K_{1-x}Bi_xF_{2x+1}$  from the work by Matar *et al.*,<sup>8</sup> where it was assumed that the conductivity thermal dependency is in the exponential term only, we see that our compound in particular has a higher conductivity with a correspondingly lower activation energy.

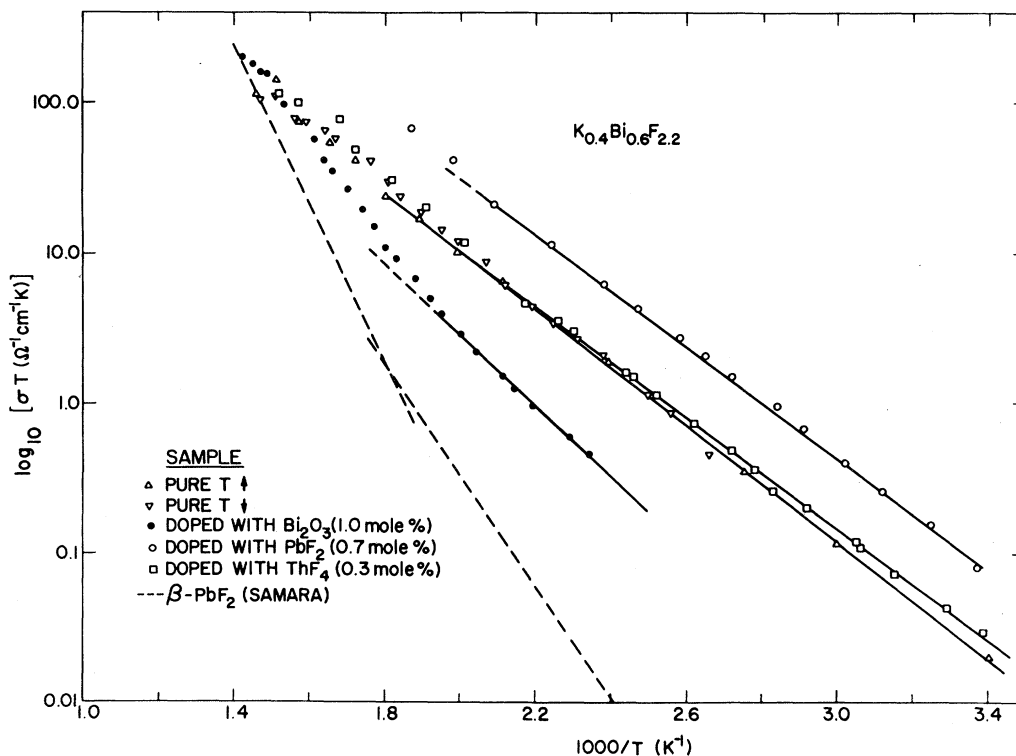


FIG. 1. Logarithm of the conductivity-temperature product  $\sigma T$  for pure and doped crystals of  $K_{0.4}Bi_{0.6}F_{2.2}$  vs  $1000/T$ , where  $T$  is absolute temperature. Undoped curves are shown for both increasing and decreasing  $T$ . For comparison, results for  $PbF_2$  from Ref. 6 are shown as a dashed line. Solid lines drawn are a guide to the eye.

TABLE I. Prefactors  $\sigma_0$  ( $10^3 \Omega^{-1} \text{cm}^{-1} \text{K}$ ) and apparent activation energies  $Q$  (eV) for a pure sample and samples doped with  $PbF_2$ ,  $ThF_4$ , and  $Bi_2O_3$ .

Sample	Pure	Pb			Th		O	
		0.4 mol %	0.7 mol %	1.5 mol %	0.3 mol %	0.65 mol %	1.3 mol %	1 mol %
$\sigma_0$	93±6	57.4±1	123±8	203±25	66±7	20±4	20±4	140±5
$Q$	0.389±0.002	0.355±0.007	0.369±0.002	0.371±0.004	0.373±0.003	0.36±0.01	0.336±0.006	0.46±0.01

Both Pb and Th impurities were found to increase the total conductivity (see Fig. 1 and Table I), whereas the apparent activation energies were slightly decreased. As for the oxygen doping, the total conductivity decreased with a moderate increase in the apparent activation energy.

The defects specific to the defective structure of this compound affect the anion sublattice and are of the Frenkel type.<sup>8</sup> Examining the ionic radius<sup>10</sup> of the dopant and of the host ions we see that  $Pb^{2+}$  can replace  $K^+$  as well as  $Bi^{3+}$ ,  $Th^{4+}$  can replace  $Bi^{3+}$  only, and  $O^{2-}$  will replace  $F^-$ . We can expect, for a low defect concentration, that a substitution of either  $Pb^{2+}$  for  $K^+$  or  $Th^{4+}$  for  $Bi^{2+}$  will increase the interstitial fluoride-ion concentration and the substitution of either  $Pb^{2+}$  for  $Bi^{2+}$  or  $O^{2-}$  for  $F^-$  will increase the fluoride-ion vacancy concentration. Depending on which type of defect is more mobile, the conductivity increases or decreases upon doping, and for a low dopant concentration it is expected that an increase in the dopant concentration (responsible for the increase of the conductivity) results in an increase in the mobile-ion content whereas the apparent activation energy is constant and coincides with the migration enthalpy. However, as in the case of the fluoride-structured solid solutions  $Ca_{1-x}Y_xF_{2x+2}$  (Ref. 11) and  $Pb_{1-x}Bi_xF_{2x+2}$  (Ref. 12), one can expect that a large concentration of point defects will be present in  $K_{0.4}Bi_{0.6}F_{2.2}$  for local charge compensation, the majority of these defects in the form of aggregates, so that the introduction of additional defects through doping may not increase the mobile-ion content. Considering that the concentration of thermally generated defects is not significant compared to the concentration of the defects already present for temperatures ranging from RT to  $\sim 250^\circ\text{C}$ , the apparent activation energy will coincide with the migration enthalpy of free defects. Both impurities Pb and Th decrease the activation energy (see Table I) but, whereas an increase in the Pb concentration results in an increase in  $Q$ , an increase in the Th concentration results in a decrease in  $Q$ .

The results show that the higher conductivities displayed by the samples doped with Pb are related to a higher prefactor,  $\sigma_0$ , which is proportional to the number of mobile defects. (Actually, the mobile-ion content decreased for the Pb concentration of 0.4 mol %, but this decrease was overcompensated by a decrease in the activation energy.)

The behavior of the  $K_{0.4}Bi_{0.6}F_{2.2}$  conductivity upon doping with the impurities Pb, Th, and O can be explained by the hypothesis<sup>13,14</sup> that the aggregates of point defects decrease the migration energy barriers of free interstitials. In the case of Th doping, for example, interstitials created by the substitution of Th for Bi would form aggregates with interstitials that were formerly free resulting in a decrease in the mobile-ion content and in a lowering of the energy barriers. Inversely, for O doping, interstitials formerly taking part in aggregates are now free but the energy barriers are higher. The distinct behavior of the samples doped with Pb from the samples doped either with Th or O is not at all unexpected, since the nature (polarizability, valence) of the dopant ion can affect the defect-defect interaction and consequently the conductivity.

A phase transition around  $300^\circ\text{C}$  has been observed in our conductivity results. There is a negative deviation in the conductivity curve, the activation energy changing from 0.389 in the low-temperature range to 0.32 eV at temperatures higher than  $300^\circ\text{C}$ . Thermal hysteresis is also observed. The existence of this phase transition was confirmed by differential thermal analysis (DTA). Data for a  $K_{0.4}Bi_{0.6}F_{2.2}$  sample were taken with a DuPont 990 Thermal Analysis System, 1600 DTA Cell and are shown in Fig. 2. The sample was sealed in a platinum tube and the heating rate was  $20^\circ\text{C}/\text{min}$ . In addition to the phase transition with a peak at  $\sim 300^\circ\text{C}$ , weaker events at higher temperatures were also observed.

Superionic conductors have been divided into two classes,<sup>15</sup> depending on whether they exhibit a first-order transition (e.g., AgI,  $YF_3$ ) where the conductivity increases by several orders of magnitude, or a

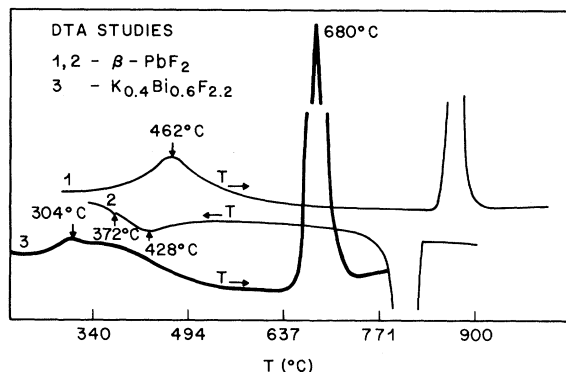


FIG. 2. DTA data are plotted for both  $\beta$ - $\text{PbF}_2$  (curves 1 and 2) and  $\text{K}_{0.4}\text{Bi}_{0.6}\text{F}_{2.2}$  (curve 3), showing peaks below the melting point which are attributed to disordering of the  $\text{F}^-$  sublattice in both cases.

diffuse transition as with the binary compounds having the fluorite structure ( $\beta$ - $\text{PbF}_2$ ,  $\text{BaF}_2$ ). In the latter case the conductivity is continuous at the transition temperature, but the activation energy falls to a value close to the values observed for superionic conductors, i.e., 0.2–0.3 eV.

It is interesting to compare the results for  $\text{K}_{0.4}\text{Bi}_{0.6}\text{F}_{2.2}$  with the results for compounds belonging to the second class, particularly  $\beta$ - $\text{PbF}_2$ , since this compound has the highest ionic conductivity at RT and the lowest transition temperature of the fluorite-structured binary compounds. DTA data for a  $\beta$ - $\text{PbF}_2$  sample (same conditions as for  $\text{K}_{0.4}\text{Bi}_{0.6}\text{F}_{2.2}$ ) show a broad but well-defined phase transition with a peak at 462°C (see Fig. 2) on warming and at 428°C upon cooling. Since the melting point of  $\text{K}_{0.4}\text{Bi}_{0.6}\text{F}_{2.2}$  is considerably below that of  $\beta$ - $\text{PbF}_2$  one might expect the phase transition to occur at a temperature low than 462°C. This was found to be the case. In addition, the electrical conductivity of  $\text{K}_{0.4}\text{Bi}_{0.6}\text{F}_{2.2}$  is several orders of magnitude higher than the electrical conductivity of  $\beta$ - $\text{PbF}_2$  at lower temperatures (see Fig. 1); this effect can be attributed to the disordered structure of  $\text{K}_{0.4}\text{Bi}_{0.6}\text{F}_{2.2}$  present even at low temperatures. Also, the transition to the superionic state might be expected to be rather muted as compared with  $\beta$ - $\text{PbF}_2$  because of the disordered nature of the low-temperature state of the crystals.

#### NMR STUDIES

The  $^{19}\text{F}$  nuclear relaxation times  $T_1$  and  $T_2$  (spin echo) have been studied as a function of temperature at an NMR frequency of 17.4 MHz. The results, shown in Fig. 3, are seen to be qualitatively similar

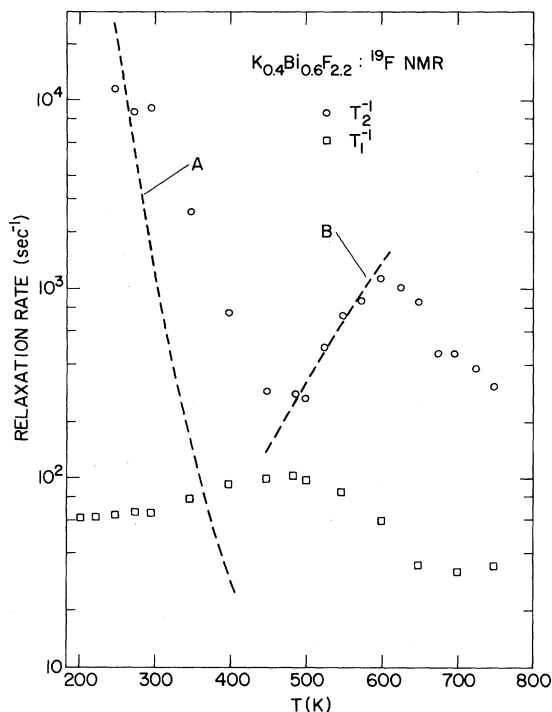


FIG. 3. Nuclear relaxation rates  $T_1^{-1}$  and  $T_2^{-1}$  (spin echo) for  $^{19}\text{F}$  in  $\text{K}_{0.4}\text{Bi}_{0.6}\text{F}_{2.2}$  are plotted on a semilogarithmic scale vs  $T$ . The dashed curves are calculated as described in the text.

to those reported for nominally pure  $\text{PbF}_2$  by Boyce *et al.*<sup>3</sup> and for Mn-doped  $\text{PbF}_2$  by Vernon *et al.*<sup>7</sup> As in these cases, most of the  $^{19}\text{F}$  relaxation behavior in  $\text{KBiF}_4$  is attributable to slow-relaxing magnetic impurities such as  $\text{Mn}^{2+}$  and  $\text{Fe}^{3+}$ . These ions are stray impurities in our  $\text{KBiF}_4$  crystals, where, for example, semiquantitative analysis shows Fe to be present in the 1–10 ppm concentration range. As detailed below, however, there are a number of contrasts between our results and those for  $\text{PbF}_2$  which reveal surprising and important features of the ionic conduction process in  $\text{KBiF}_4$ .

We begin by discussing the (upper) curve of  $T_2^{-1}$  vs  $T$  in Fig. 3. At the lowest temperatures ( $T < 300$  K) the  $T_2$  decay process is caused by  $^{19}\text{F}$ - $^{19}\text{F}$  and to a lesser extent by  $^{19}\text{F}$ - $^{209}\text{Bi}$  nuclear dipolar interactions. The overall decay process is not exponential; the values plotted in Fig. 3 are from a roughly exponential tail ( $t \rightarrow \infty$ ) on the decay function. When the fluorine hopping frequency  $\tau_F^{-1}$  begins to exceed  $T_2^{-1}$  (static), the  $^{19}\text{F}$  NMR line becomes motionally narrowed, with an exponential decay constant<sup>7</sup>

$$T_2^{-1} = \langle (\Delta\omega)^2 \rangle \tau_F, \quad (3)$$

where  $\langle (\Delta\omega)^2 \rangle$  is the dipolar second moment of the line. To estimate  $T_2$  with Eq. (3) we may calculate  $\langle (\Delta\omega)^2 \rangle$  to good accuracy and estimate the hopping frequency from the conductivity using the Nernst-Einstein relation. Denoting the latter estimate  $\tau_{F\sigma}^{-1}$ , one has

$$\tau_{F\sigma} = Nd^2e^2/6\sigma k_B T, \quad (4)$$

where  $N$  is the volume density of  $F^-$  ions and  $d$  is the jump distance, taken to be the  $F^-$ - $F^-$  nearest-neighbor distance.

For  $PbF_2$  the foregoing scheme leads to an excellent estimate of the narrowed  $T_2$  behavior.<sup>3</sup> For  $KBiF_4$ , however, the estimate of  $T_2^{-1}$  taking  $\tau_F = \tau_{F\sigma}$  [Eqs. (3) and (4)], shown as dashed line *A* in Fig. 3, is grossly in error. Since we believe Eq. (1) to be fundamentally correct, the error apparently lies in assuming  $\tau_F = \tau_{F\sigma}$ . The sense of this error is such that the conductivity greatly overestimates the hopping frequency of the majority of  $F^-$  ions. It follows that the ionic conduction in  $KBiF_4$  is dominated by "easy" conduction paths which constitute only a small fraction of the crystal volume. We also conclude that there is a wide distribution of jump frequencies at any temperature.

Above  $T \sim 500$  K, values of  $T_2^{-1}$  in Fig. 3 are seen to increase again, marking the onset of the magnetic impurity-generated "encounter" relaxation process. This process has been analyzed in detail by Vernon *et al.*<sup>7</sup> to be a function of the concentration  $c$ , spin-lattice relaxation time  $\tau_{sl}$  of the magnetic impurities, the hyperfine coupling parameter<sup>16</sup>  $A_{zz}$ , and the fluorine hopping rate  $\tau_F^{-1}$ . At low temperatures the encounter process is one in which the phase of fluorine nuclear motion becomes totally "scrambled" each time it comes into a "cell" of sites surrounding a magnetic impurity, so that  $(T_2^{-1})_{enc}$  becomes simply the average rate at which  $F^-$  ions encounter such a cell. Thus

$$(T_2^{-1})_{enc} = zc/\tau_F W, \quad (5)$$

where  $z(=4)$  is the cation coordination number of an F site and  $W$  describes a geometrical effect representing paths of motion which begin and end on sites neighboring the same impurity. Vernon *et al.*<sup>7</sup> calculate  $z/W \sim 1$  for the fluorite lattice. As temperature is increased, however, the hyperfine

coupling effect during the encounter eventually becomes "narrowed" by the shortness of  $\tau_F$  or  $\tau_{sl}$  or both and  $T_2^{-1}$  again declines, as seen in Fig. 3.

We may apply Eq. (5) to the rising portion of the  $T_2^{-1}$  curve in Fig. 3 by again taking  $\tau_F = \tau_{F\sigma}$  [Eq. (2)] and adjusting  $c$  to make a reasonable fit. The result is dashed curve *B* in Fig. 3, which is seen to have a roughly correct temperature dependence over the range from 500 to 600 K. However, for this curve  $c$  is only  $\sim 0.3$  ppm, which is roughly an order of magnitude less than the known impurity level. This discrepancy supports our earlier finding that  $\tau_{F\sigma}^{-1}$  overestimates the  $F^-$  hopping frequency by an order of magnitude or more. By contrast, Eq. (5) is found to give reasonable agreement with Mn-doped  $PbF_2$ .<sup>7</sup> It is interesting to compare our  $T_2^{-1}$  curve in Fig. 3 with that for Mn-doped  $PbF_2$  with  $c = 150$  ppm (Ref. 7, Fig. 3). Both curves have maxima at  $T \sim 600$  K, but differ in their peak values by a factor of  $\sim 30$ . The similarity of these curves and the established linearity of  $(T_2^{-1})_{enc}$  with concentration<sup>7</sup> again suggests a magnetic impurity level  $c \sim 5$  ppm in our  $KBiF_4$  crystals, consistent with the foregoing discussion.

The  $T_1$  results were of excellent quality with precisely exponential decays extending over nearly two decades. The variation of  $T_1^{-1}$  with temperature in Fig. 3 appears to behave in a qualitatively similar fashion to Mn-doped  $PbF_2$ ,<sup>7</sup> but is actually quite different in detail. The peak in  $T_1^{-1}$  is rather muted and does not reach the minimum value of  $T_2^{-1}$ . This may be a consequence of the wide distribution of  $\tau_F$  values inferred from the  $T_2$  results, which may smear out the relatively sharp peak in  $T_1^{-1}$  observed for  $PbF_2$ . It is also quite remarkable that the  $T_1^{-1}$  curve becomes flat at low temperatures in contrast with the sharp decline observed for Mn-doped  $PbF_2$ . A simple interpretation of this effect consistent with the previous discussion would be that a minority of rapidly moving  $F^-$  ions continue to have their nuclei relaxed by the encounter mechanism, communicating this relaxation to the bulk by migrating beyond the spin-diffusion barrier radius.<sup>17</sup> It seems unlikely that the conventional relaxation mechanism by paramagnetic impurities<sup>17</sup> is important here in view of its weakness in undoped  $PbF_2$ , where the encounter mechanism effects are less than an order of magnitude smaller than in the present work, but low-temperature  $T_1$ 's are more than 3 orders of magnitude longer.

- \*Present address: Instituto de Pesquisas Energeticas e Nucleares, São Paulo, São Paulo, Brazil.
- <sup>1</sup>R. T. Harley, W. Hayes, A. J. Rushworth, and J. F. Ryan, *J. Phys. C* **8**, L530 (1975).
- <sup>2</sup>R. Benz, *Z. Phys. Chem. Neue Folge* **95**, 25 (1975).
- <sup>3</sup>J. B. Boyce, J. C. Mikkelsen, Jr., and M. O'Keeffe, *Solid State Commun.* **21**, 955 (1977).
- <sup>4</sup>R. D. Hogg, S. P. Vernon, and V. Jaccarino, *Phys. Rev. Lett.* **39**, 481 (1977).
- <sup>5</sup>H. M. Dickens, W. Hayes, C. Smith, and M. T. Hutchins, in *Fast Ion Transport in Solids*, edited by P. Vashishta, J. N. Mundy, and G. K. Shenoy (North-Holland, New York, 1979).
- <sup>6</sup>G. Samara, *J. Phys. Chem. Solids* **40**, 509 (1979).
- <sup>7</sup>S. P. Vernon, P. Thayamballi, R. D. Hogg, D. Hone, and V. Jaccarino, *Phys. Rev. B* **24**, 3756 (1981).
- <sup>8</sup>S. Matar, J.-M. Réau, C. Lucat, J. Grannec, and P. Hagenmuller, *Mater. Res. Bull.* **15**, 1295 (1980).
- <sup>9</sup>S. J. Allen, A. S. Cooper, F. DeRosa, J. P. Remeika, and S. K. Ulasi, *Phys. Rev. B* **17**, 4031 (1978).
- <sup>10</sup>R. D. Shannon and C. T. Prewitt, *Acta Crystallogr. Sect. B* **25**, 925 (1969).
- <sup>11</sup>A. K. Cheetham, B. E. F. Fender, and M. J. Cooper, *J. Phys. C* **4**, 3107 (1971); D. Steele, P. E. Childs, and B. E. F. Fender, *ibid.* **5**, 2677 (1972).
- <sup>12</sup>C. Lucat, J. Portier, J.-M. Réau, P. Hagenmuller, and J.-L. Soubeyroux, *J. Solid State Chem.* **32**, 279 (1980).
- <sup>13</sup>C. R. A. Catlow, *J. Phys. C* **9**, 1859 (1976).
- <sup>14</sup>K. E. D. Wapenaar and J. Schoonman, *J. Electrochem. Soc.* **126**, 667 (1979).
- <sup>15</sup>M. O'Keeffe and B. G. Hyde, *Philos. Mag.* **33**, 219 (1976).
- <sup>16</sup>The hyperfine interaction is written  $A_{zz}I_zS_z + A_{\pm}(I_+S_- + I_-S_+)$ .
- <sup>17</sup>G. R. Khutsishvili, *Zh. Eksp. Teor. Fiz.* **31**, 424 (1956) [*Sov. Phys.—JETP* **3**, 382 (1957)]; P. G. de Gennes, *J. Phys. Chem. Solids* **7**, 345 (1958).